Supporting Information

Experimental Section

Materials and Measurements.

All reagents of analytical grades were purchased commercially and used without further purification. Nuclear magnetic resonance (NMR) data were collected on Bruker AVANCE III 400 (400 MHz) Spectrometer. IR experiments were tested using Nicolet/Nexus-670 FT-IR spectrometer in the region of 4000-400 cm^{-1}. The tablet samples were compressed by a Mini-Pellet Press of Specac. Powder X-ray diffraction (PXRD) patterns were recorded by a Rigaku SmartLab diffractometer (Bragg-Brentano geometry, Cu Kα1 radiation, λ = 1.54056 Å). Thermogravimetric analysis (TGA) was performed on a NETZSCH TG209 system in nitrogen and under 1 atm of pressure at a heating rate of 5 °C min^{-1}. Fluorescence microscopy photos were taken under a UV lamp using UV radiation of 365 nm. Fluorescence spectra were recorded with Edinburgh FLS 980 spectrometer. Time-gated spectra were measured by PerkinElmer LS-55. Photoluminescence quantum yields were obtained using Hamamatsu C9920-02G absolute PL quantum yield measurement system. The long persistent luminescence (LPL) spectra were tested on an Ocean Optics spectrophotometer (QE65 Pro) using 365 nm, 405 nm and white light from the flashlight as the excitation light sources, respectively. The measurements were carried out in high-velocity scanning mode of QE65 pro with integration time of 8 ms and scanning time of 10 s.

X-ray single crystal structure analysis

Single-crystal X-ray diffraction data for H_2TzPCz and LIFM-ZCY-1 were collected on a Rigaku Oxford SuperNova X-RAY diffractometer system equipped with a Cu sealed tube (λ = 1.54178 Å) at 50 kV and 0.80 mA. The structure was solved by direct methods, and refined by full-matrix least-square methods with the SHELXL-2014 program package. All hydrogen atoms were located in calculated positions and refined anisotropically. The single crystal data have been deposited in the Cambridge Crystallographic Data Center (CCDC No: 1990481-1990482).

Theoretical calculations

Molecular geometries were extracted in single crystals and performed by Gaussian 09 package with time-dependent density functional theory (TD-DFT) with Beck's three-parameter hybrid exchange functional [S1] and Lee, and Yang and Parr correlation functional [S2] (B3LYP) with 6-311G(d) basic set. The SCF convergence was 10^{-8} a.u. while the gradient and energy convergence were 10^{-4} a.u. and 10^{-5} a.u., respectively.

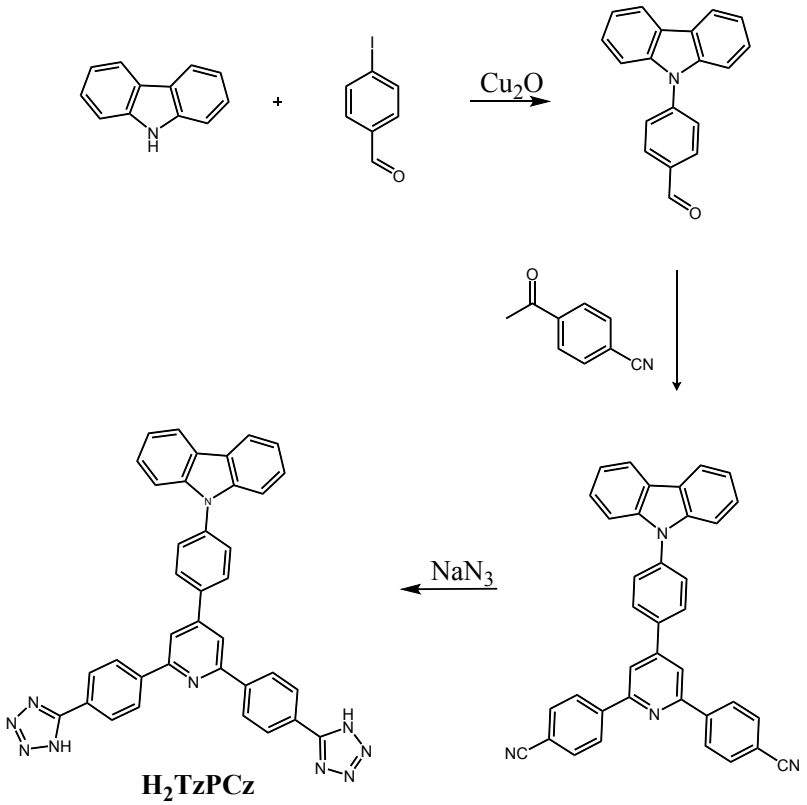

Scheme S1. Synthesis route of H_2TzPCz.

Synthesis of 4-(Carbazol-9-yl) benzaldehyde: product was prepared from carbazole and 4-Iodobenzaldehyde following the reported procedure.

Synthesis of 4,4'-(4-(4-(9H-carbazol-9-yl)phenyl)pyridine-2,6-diyl)dibenzonitrile: A solution of p-Cyanacetophenon (40 mmol), 4-(Carbazol-9-yl) benzaldehyde (20 mmol) and NaOH (40 mmol) in 200 mL ethanol was stirred for about 15 hours at room temperature after which aqueous ammonia (80 mL) was added and stirred for another 24 hours at room temperature. After the solvent was moved, the residue was purified by column chromatography (petroleum ether/CH_2Cl_2, V/V = 1: 2) to afford 4.0g light yellow solid with 38% yield. ^{1}H NMR (DMSO-d6, 400 MHz): δ (ppm) 8.62 (d, 4H), 8.59 (s, 2H), 8.44(d, 2H), 8.30(d, 2H), 8.06(d, 2H), 7.87(d, 2H), 7.51(m, 4H), 7.39(m, 2H).

Synthesis of 9-(4-(2,6-bis(4-(1H-tetrazol-5-yl) phenyl) pyridin-4-yl) phenyl)-9H-carbazole (H_2TzPCz): Into a 25 mL round-bottomed flask were added sodium azide (1.12 g, 16 mmol) and 2 mL of water. 4,4'-(4-(4-(9H-carbazol-9-yl) phenyl) pyridine-2,6-diyl) dibenzonitrile (2 mmol) was dissolved in 10 mL of *N*-Methylpyrrolidone and injected into the solution. The reaction mixture was refluxed for 24 h with vigorous stirring at 150^{o}C. The mixture was acidified to pH 1 with aqueous HCl solution (1 M), the tetrazole product precipitated upon stirring, which was extracted into 20 mL ethyl acetate and the organic layer was separated. The aqueous layer was washed with ethyl acetate. The organic layers were combined, concentrated and dried under vacuum to

yield white solid product. ^{1}H NMR (DMSO-d_6, 400 MHz): δ (ppm) 8.61 (m, 6H), 8.43 (d, 2H), 8.29 (d, 2H), 8.06 (d, 2H), 7.87 (d, 2H), 7.50 (m, 4H), 7.34 (m, 2H). ESI-MS: calc. for [M+H$^+$] 609.22, found: 609.34. IR (KBr, cm^{-1}): 3442(b), 3039(w), 2918(w), 2851(w), 2722(w), 2610(w), 2557(w), 2457(w), 1597(s), 1542(w), 1518(m), 1503(w), 1480(w), 1451(s), 1421(w), 1395(w), 1359(w), 1333(w), 1318(w), 1224(w), 1172(w), 1151(w), 1113(w), 1066(w), 1037(w), 1019(w), 998(w), 910(w), 828(m).

Synthesis of LIFM-ZCY-1 ($[Cd(TzPCz)(DMA)_2(H_2O)_6]_n$**)**: A mixture of $CdCl_2$ (10 mg, 0.03 mmol) and H_2TzPCz (5 mg, 0.005 mmol) dissolved in the mixture of 1 mL of N, N-Dimethylacetamide (DMA), 0.5 mL of deionized water and 1 mL of ethanol. The mixture was sealed in a 10 ml glass vessel and heated at 90 ^{o}C for two days and then slowly cooled to room temperature naturally. Laminar single crystals of LIFM-ZCY-1 were collected with the yield of 70%. IR (KBr, cm^{-1}): 3413(b), 2925(w), 2850(w), 2808 (w), 1629(s), 1602(s), 1543(w), 1516(m), 1478(w), 1451(m), 1428(w), 1413(w), 1396(w), 1363 (w), 1337(s), 1323(w), 1228(w), 1175(w), 1158(w), 1132(w), 1113(w), 1043(w), 1022(w), 1008(w), 963(w), 912(w), 858(m), 838(w), 770(w).

Transformation to LIFM-ZCY-1': LIFM-ZCY-1 was heated to 460 K and then cooled back to room temperature (300 K), while the solvent-escaped structural transformation was kept and named as LIFM-ZCY-1'. Different from LIFM-ZCY-1, LIFM-ZCY-1' has a dense coordination structure, which genders the appearance of long persistent luminescence. IR (KBr, cm^{-1}): 3427(b), 3073(w), 2925(w), 2859(w), 1599(s), 1540(w), 1517(m), 1476(w), 1447(s), 1424(w), 1394(w), 1365(w), 1333(w), 1315(s), 1280(w), 1245(w), 1225(w), 1172(w), 1120(w), 1081(w), 1037(w), 994(w), 915(w), 888(w), 851(m), 836(w).

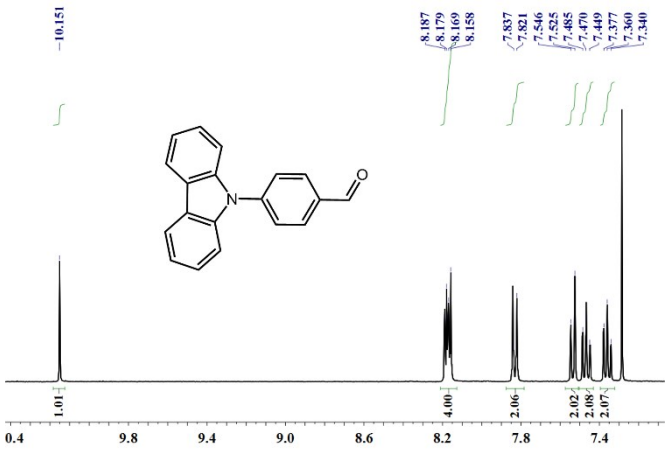

Figure S1. [1]H NMR spectrum of 4-(Carbazol-9-yl) benzaldehyde.

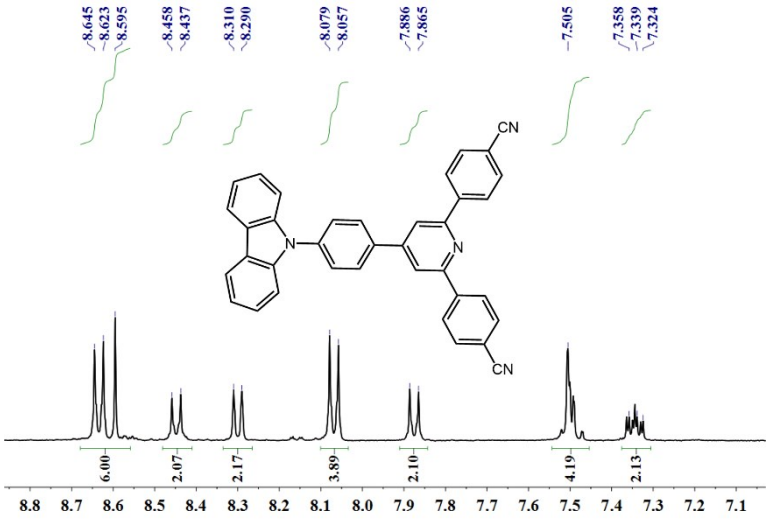

Figure S2. [1]H NMR spectrum of 4,4'-(4-(4-(9H-carbazol-9-yl) phenyl) pyridine-2,6-diyl) dibenzonitrile.

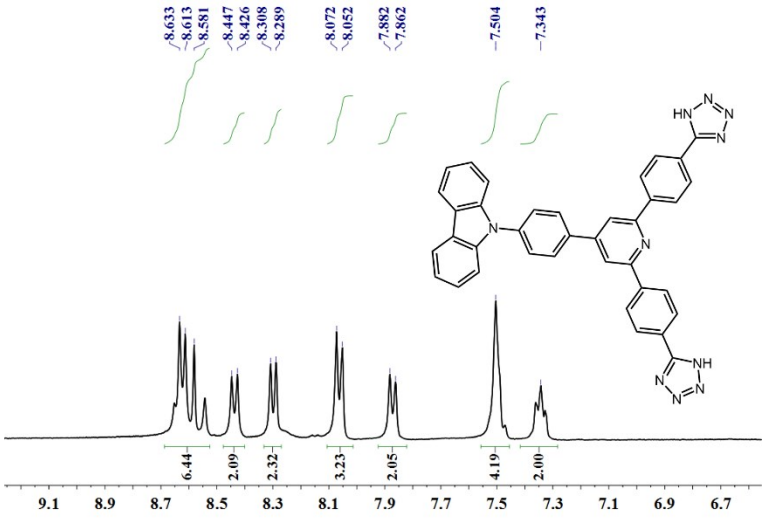

Figure S3. [1]H NMR spectrum of H_2TzPCz.

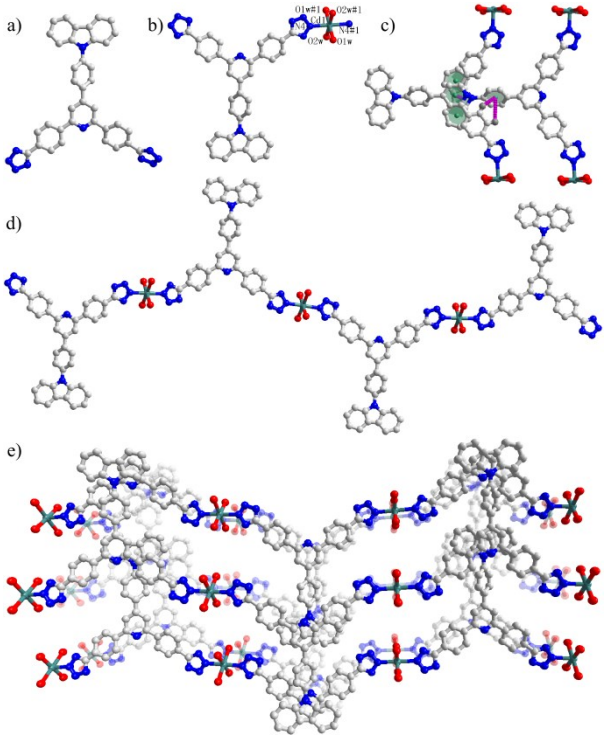

Figure S4. a) The structure of H_2TzPCz. b) Asymmetric unit and coordination surrounding of LIFM-ZCY-1 (the hydrogen atoms and solvent molecules are omitted). c) π...π stacking and C-H...π interactions (pink dot line). d) 1D chain formed by coordination self-assembly. f) 3D network formed by 1D chains via π...π stacking and C-H...π interactions.

Table S1. Crystal data and structure refinement for LIFM-ZCY-1

Empirical formula	$C_{45}H_{60}N_{12}O_{12}Cd$
Formula weight	1073.45
Crystal system	monoclinic
Space group	C2/c
a/Å	6.9834(4)
b/Å	17.4254(8)
c/Å	39.8368(17)
α/°	90
β/°	91.782(4)
γ/°	90
Volume/Å^3	4845.3(4)
Z	4
Calculated density	1.472
Temperature/K	150.15(10)

F(000)	2232.0
Radiation	CuKα (λ = 1.54184)
Theta range for data	8.884 to 87.268
Limiting indices	$-6 \le h \le 6$, $-15 \le k \le 15$, $-35 \le l \le 35$
Reflections collected	5898
Independent reflections	1803 [R_{int} = 0.0425, R_{sigma} =0328]
Data/restraints/parameters	1803/118/323
Quality-of-fit indicator	1.144
Final *R* indices [$I>2\sigma(I)$]	R_1 = 0.1113, wR_2 = 0.2647
R indices (all data)	R_1 = 0.1152, wR_2 = 0.2670
Largest diff. peak and hole	1.51/-0.54 e.Å^{-3}

Table S2. Crystal data and structure refinement for H_2TzPCz

Empirical formula	$C_{43}H_{38}N_{12}O_2$
Formula weight	754.85
Crystal system	monoclinic
Space group	$P2_1/c$
a/Å	15.1225(2)
b/Å	31.4203(5)
c/Å	7.93350(10)
α/°	90
β/°	92.9100(10)
γ/°	90
Volume/Å^3	3764.77(9)
Z	4
Calculated density	1.332
Temperature/K	150.01(10)
F(000)	1584.0
Radiation	CuKα (λ = 1.54184)
Theta range for data	8.12 to 132.01
Limiting indices	$-17 \le h \le 17$, $-35 \le k \le 37$, $-6 \le l \le 9$
Reflections collected	15204
Independent reflections	6557 [R_{int} = 0.0247, R_{sigma} = 0.0275]

Data/restraints/parameters	6557/0/522
Quality-of-fit indicator	1.035
Final *R* indices [$I>2\sigma(I)$]	$R_1 = 0.0460$, $wR_2 = 0.1230$
R indices (all data)	$R_1 = 0.0553$, $wR_2 = 0.1326$
Largest diff. peak and hole	0.22/-0.25 e.Å^{-3}

Table S3. Selected bond distances (Å) for H_2TzPCz and LIFM-ZCY-1

H_2TzPCz			**LIFM-ZCY-1**		
Atom 1	**Atom 2**	**Bond distances (Å)**	**Atom 1**	**Atom 2**	**Bond distances (Å)**
O1	C38	1.242(3)	Cd1	O1W	2.269(11)
N11	C38	1.312(3)	Cd1	O2W	2.312(11)
N11	C39	1.448(3)	Cd1	N4	2.258(8)
N11	C40	1.458(3)	O1	C23	1.35(2)
O2	C41	1.238(3)	N7	C21	1.516(18)
N12	C41	1.309(3)	N7	C22	1.46(2)
N12	C42	1.448(3)	N7	C23	1.15(2)
N12	C43	1.444(3)	N1	C6	1.418(12)
N1	N2	1.348(2)	N1	C7	1.402(18)
N1	C1	1.336(2)	N6	C20	1.311(13)
N2	N3	1.292(3)	N2	C13	1.330(11)
N3	N4	1.367(2)	N3	N4	1.357(12)
N4	C1	1.315(2)	N3	C20	1.311(12)
N5	C8	1.343(2)	N4	N5	1.280(11)
N5	C12	1.346(2)	N5	N6	1.346(11)
N6	N7	1.366(2)	N6	C20	1.311(13)
N6	C19	1.322(2)			
N7	N8	1.295(3)			
N8	N9	1.350(2)			
N9	C19	1.332(2)			
N10	C23	1.428(2)			
N10	C26	1.398(2)			
N10	C37	1.408(2)			

Table S4. Selected bond angles (deg) for H_2TzPCz.

Atom 1	Atom 2	Atom 3	Angle/°
C38	N11	C39	123.17(19)
C38	N11	C40	120.63(19)
C39	N11	C40	116.18(19)
O1	C38	N11	126.4(2)
C41	N12	C42	121.68(19)
C41	N12	C43	120.52(19)
C43	N12	C42	117.81(19)
O2	C41	N12	124.3(2)
C1	N1	N2	108.98(16)
N3	N2	N1	105.79(16)
N2	N3	N4	111.23(16)
C1	N4	N3	105.37(17)
C8	N5	C12	118.55(15)

Table S5. Selected bond angles (deg) for LIFM-ZCY-1.

Atom 1	Atom 2	Atom 3	Angle/°
O1W	Cd1	O1W[1]	180.0(4)
O1W[1]	Cd1	O2W	82.7(5)
O1W	Cd1	O2W	97.3(5)
O1W	Cd1	O2W[1]	82.7(5)
O2W	Cd1	O2W[1]	180.0(6)
N4	Cd1	O1W[1]	89.8(3)
N4	Cd1	O1W	90.2(3)
N4	Cd1	O2W[1]	91.2(3)
N4	Cd1	O2W	88.8(3)
N4	Cd1	N4[1]	180.0
N3	N4	Cd1	124.2(6)
N5	N4	Cd1	125.1(6)

Symmetry transformations used to generate equivalent atoms:
[1]1/2-X,1/2-Y,1-Z; [2]-X, +Y,1/2-Z.

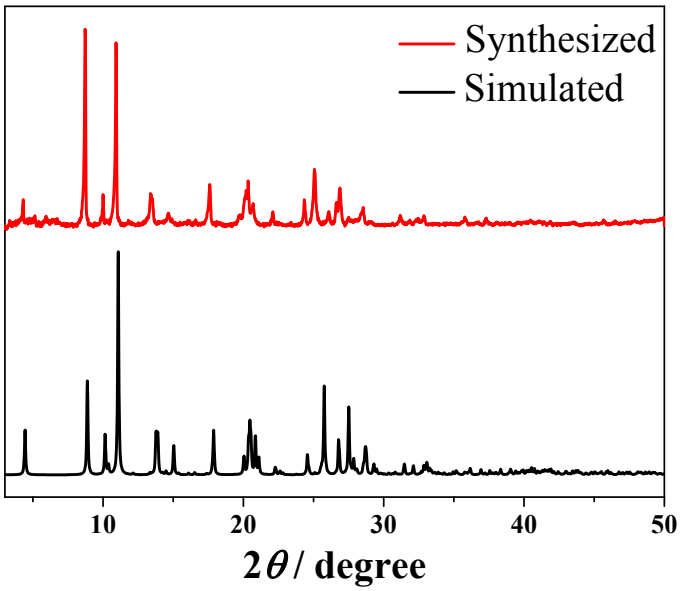

Figure S5. PXRD patterns of simulated and as-synthesized LIFM-ZCY-1.

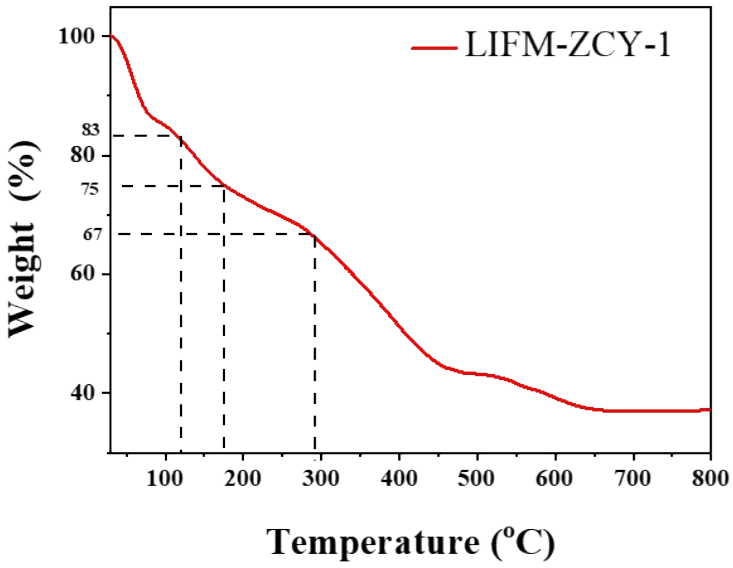

Figure S6. The TGA curves of LIFM-ZCY-1.

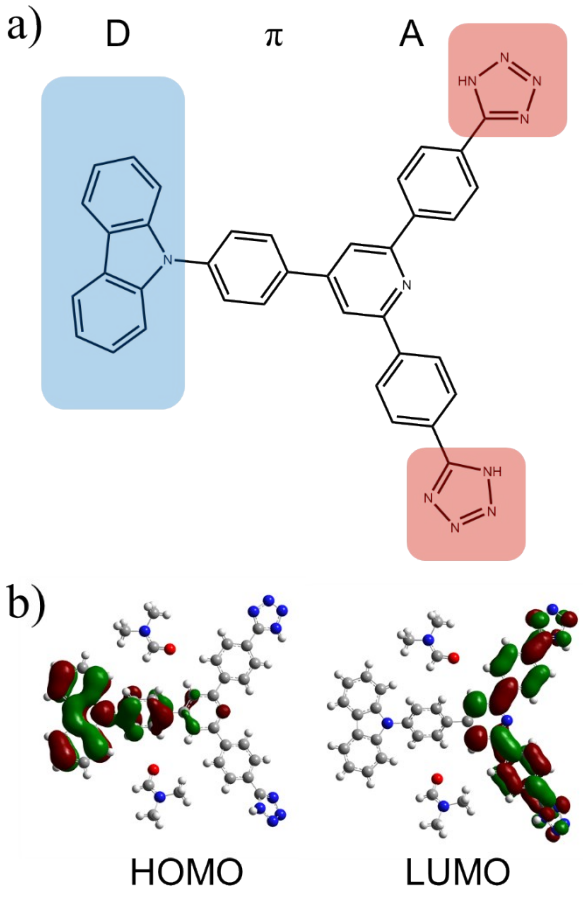

Figure S7. a) The D- π -A structure of ligand H_2TzPCz; b) The calculated HOMO and LUMO orbitals of ligand H_2TzPCz at the B3LYP/6-311G(d) level.

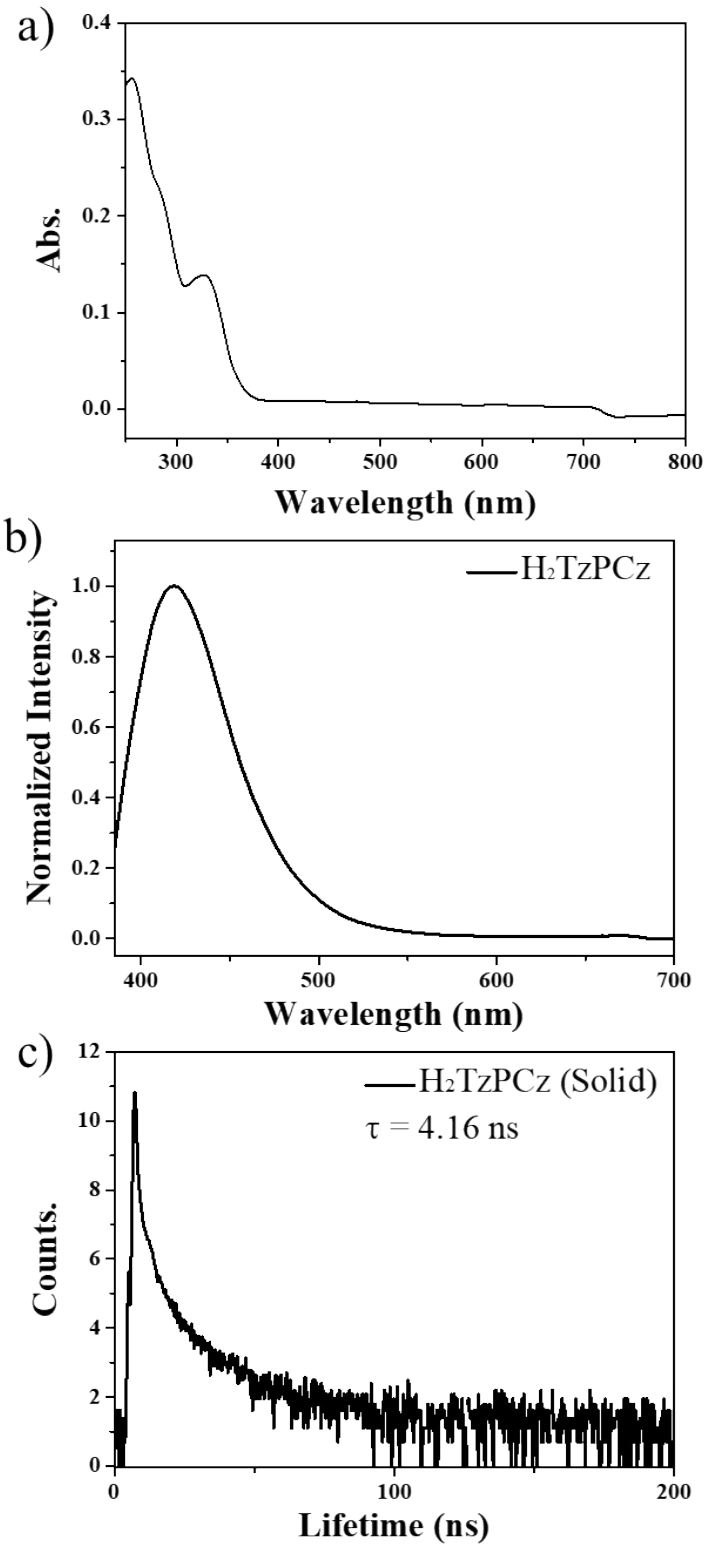

Figure S8. The photophysical properties of ligand H_2TzPCz. a) UV-Vis adsorption spectra of ligand H_2TzPCz in acetone. b) emission spectra of H_2TzPCz crystal with 365 nm excitation. c) decay curve of H_2TzPCz under 360 nm excitation.

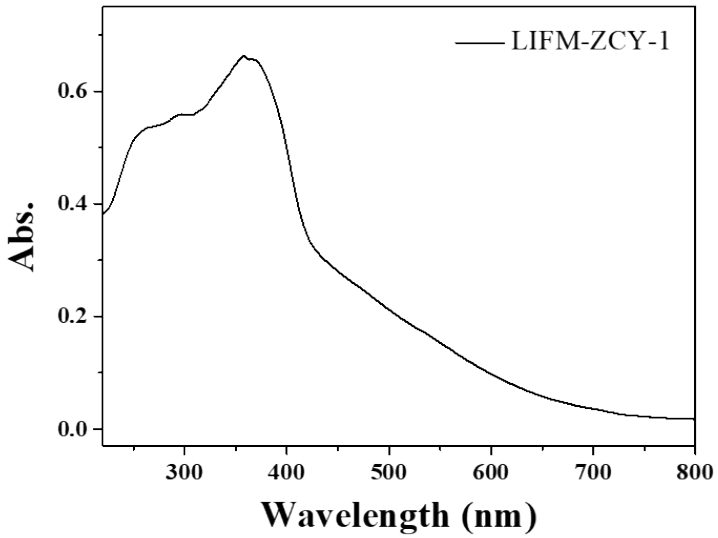

Figure S9. Solid state UV-Vis spectrum of LIFM-ZCY-1 powder.

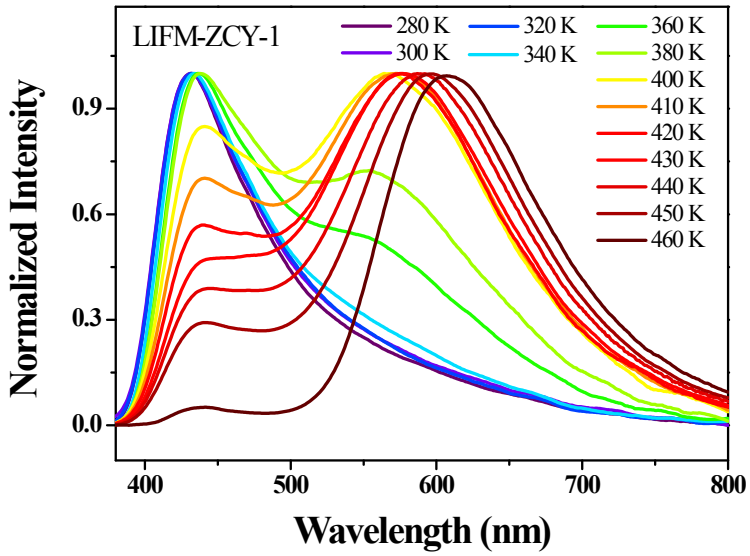

Figure S10. Temperature-dependent steady state emission spectra of LIFM-ZCY-1 from 280 to 460 K (λ_{ex} = 365 nm, solid state).

Table S6. The temperature-dependent CIE coordinates and emission maximum (λ_{max}) of LIFM-ZCY-1.

Temp.(K)	x	y	λ_{max}
280	0.2108	0.1926	431
300	0.215	0.2012	432
320	0.2123	0.2009	433
340	0.2216	0.2149	434
360	0.2634	0.2732	437
380	0.2901	0.3051	438
400	0.3369	0.3523	564
410	0.354	0.3683	572
420	0.3693	0.3825	575
430	0.383	0.3959	576
440	0.4089	0.3983	587
450	0.4411	0.4013	596
460	0.5439	0.4213	608

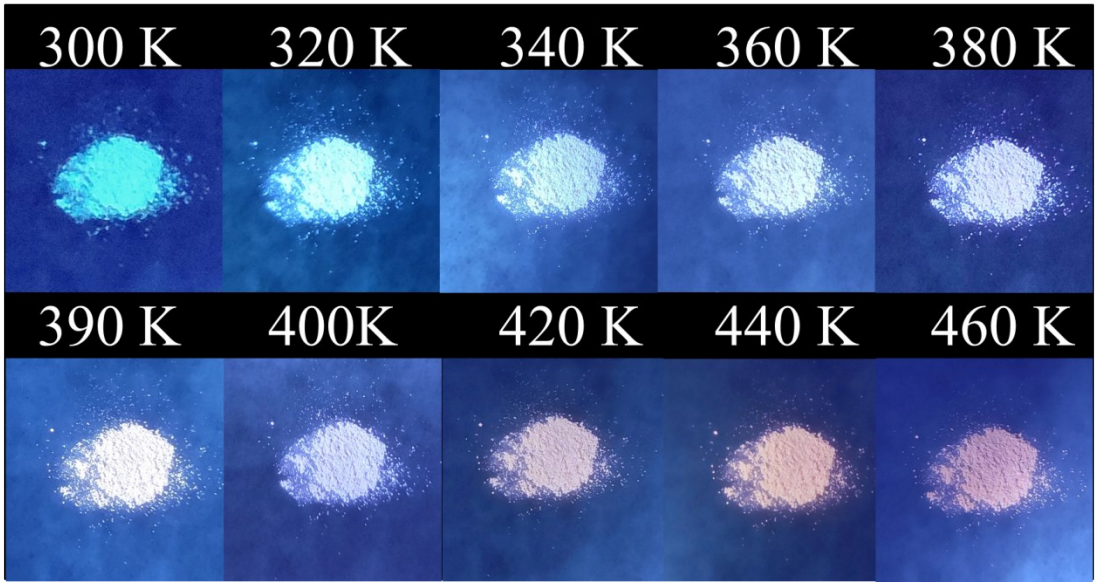

Figure S11. The emission pictures of LIFM-ZCY-1 powder under different temperature from 300 to 460 K with UV flashlight excitation.

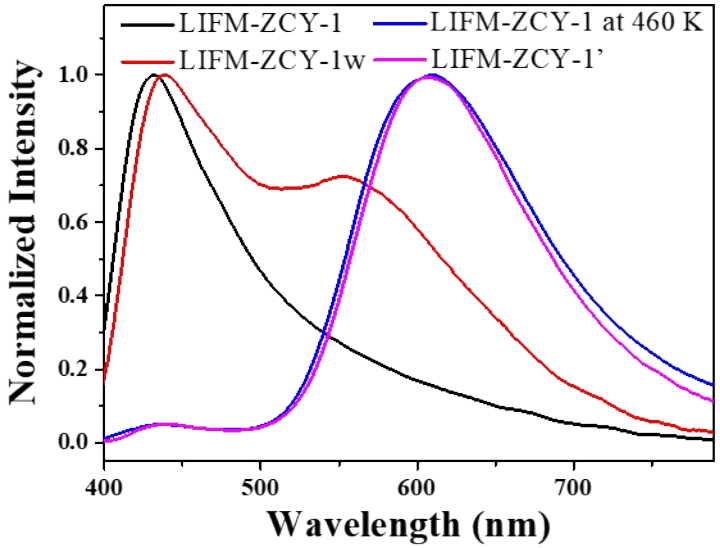

Figure S12. Steady state emission spectra (λ_{ex} = 365 nm) of LIFM-ZCY-1, LIFM-ZCY-1 at 400 K (LIFM-ZCY-1w), LIFM-ZCY-1 at 460 K, and LIFM-ZCY-1 at 460 K cooling back to 300 K (LIFM-ZCY-1').

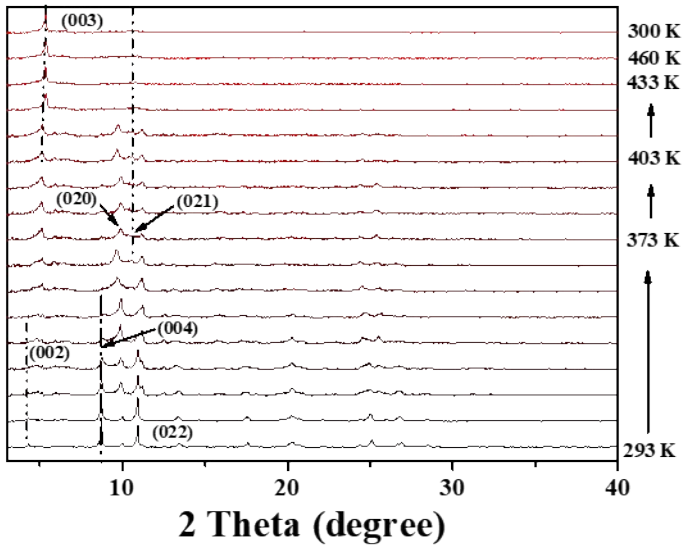

Figure S13. In-situ PXRD spectrum of LIFM-ZCY-1 from 293 K to 433 K, heating to 460 K and cooling back to 300 K.

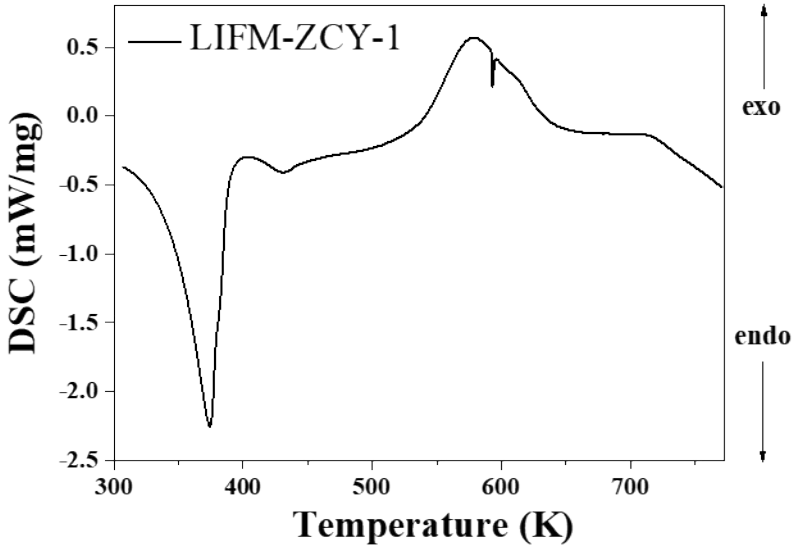

Figure S14. The DSC curves of LIFM-ZCY-1.

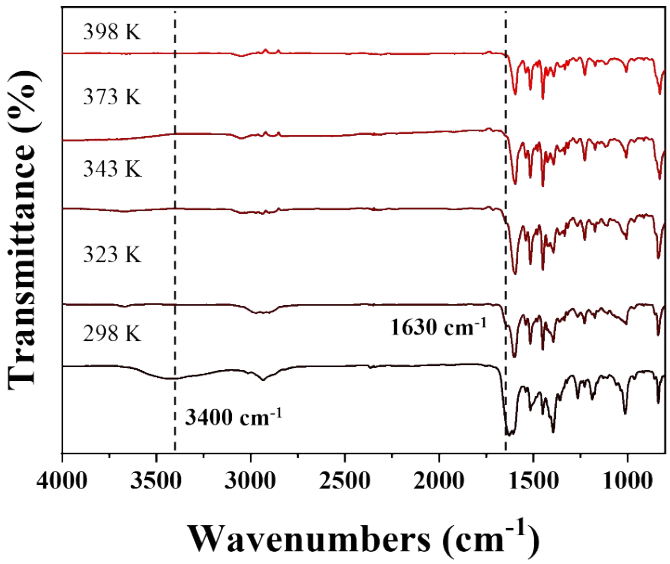

Figure S15. Temperature-dependent IR spectra of LIFM-ZCY-1 from 298 to 398 K.

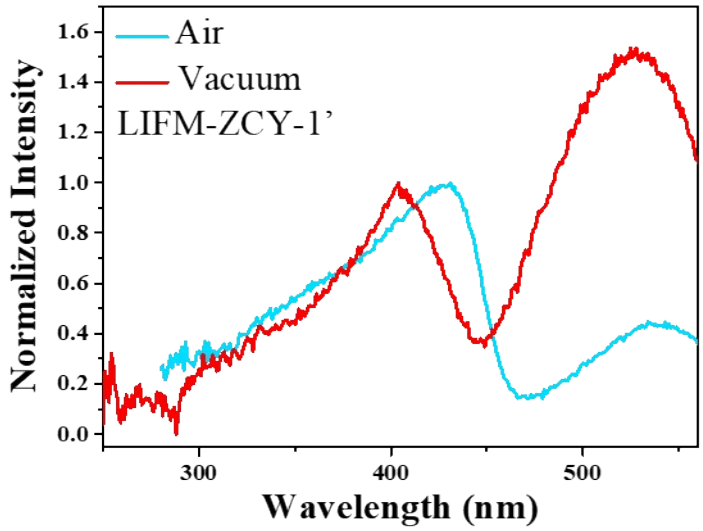

Figure S16. The excitation spectra of LIFM-ZCY-1' under vacuum and in air (λ_{em} = 620 nm).

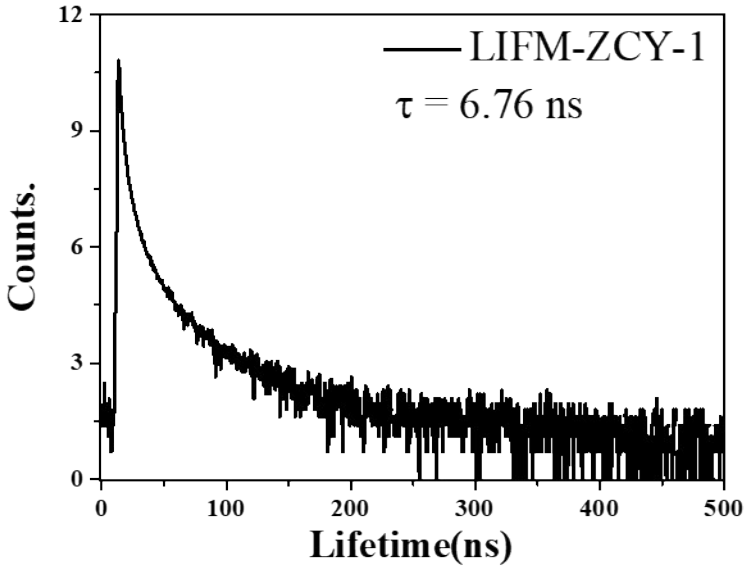

Figure S17. The decay curves of LIFM-ZCY-1 at 433 nm excited with 360 nm laser.

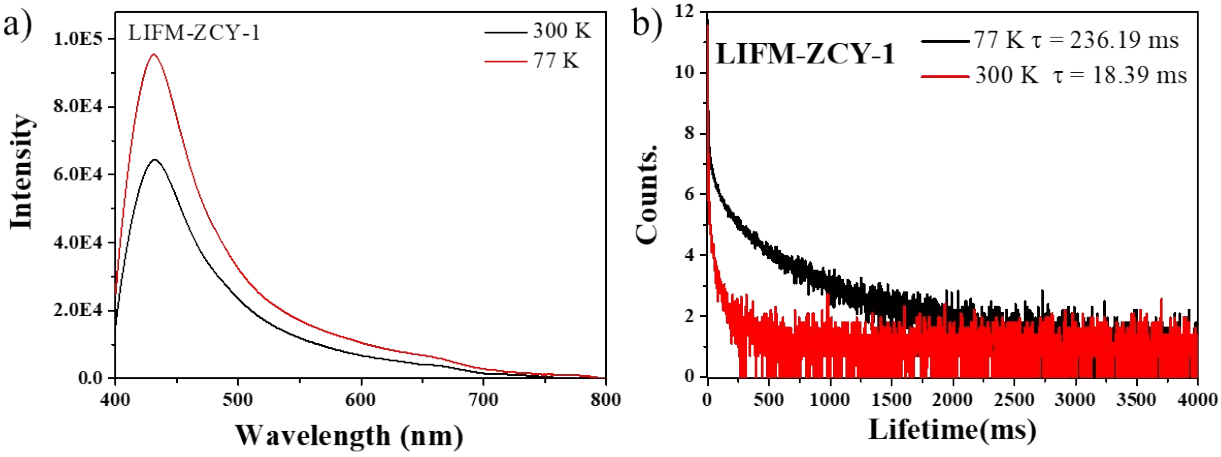

Figure S18. The emission spectra a) and decay curves at 583 nm b) of LIFM-ZCY-1 under 300 K and 77 K (λ_{ex} = 365 nm).

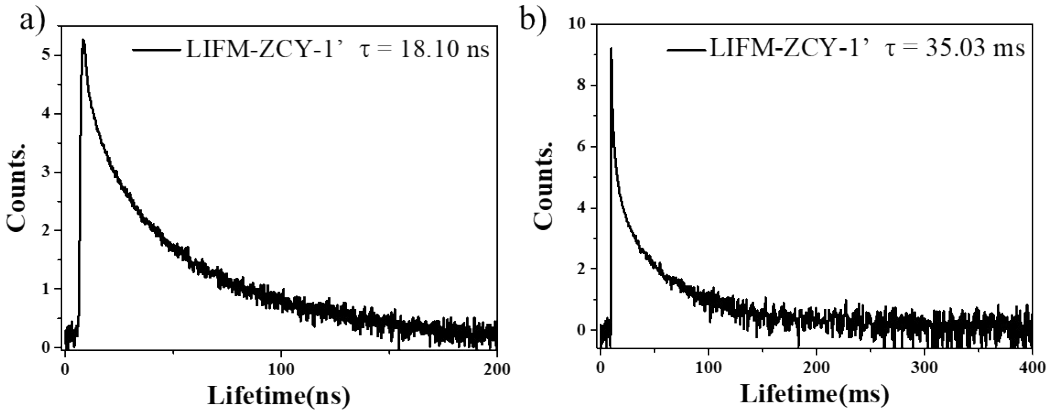

Figure S19. a) The decay curves of LIFM-ZCY-1' at 438 nm excited with 360 nm laser. b) The decay curves of LIFM-ZCY-1' at 620 nm excited with 365 nm μs lamp.

Table S7. The temperature-dependent decay lifetimes of LIFM-ZCY-1 (λ_{ex} =365 nm).

Temp.(K)	Lifetime at 450 nm (ns)	Lifetime at 570 nm (ms)
77	5.45	236.19
100	4.37	230.59
125	4.55	225.32
150	5.26	208.75
175	5.72	179.18
200	5.91	172.25
225	5.97	127.99
250	6.16	110.53
275	6.34	35.99
300	6.76	18.39

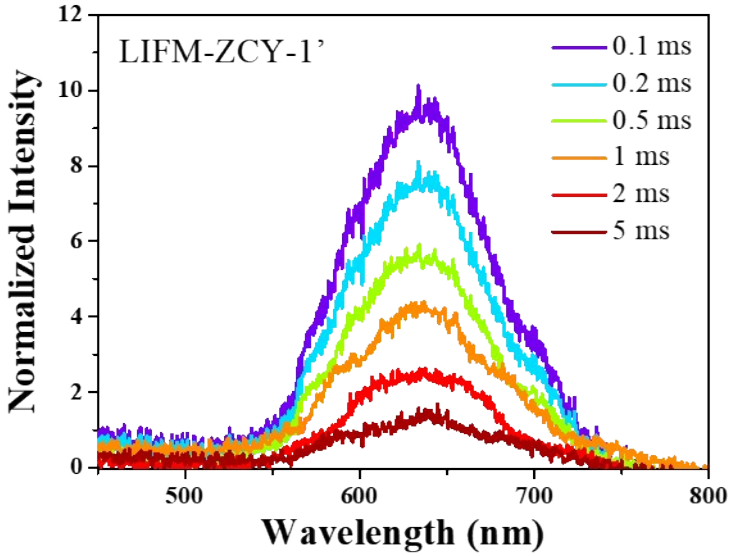

Figure S20. Time-resolved emission spectra of LIFM-ZCY-1' at 300 K under 365 nm excitation.

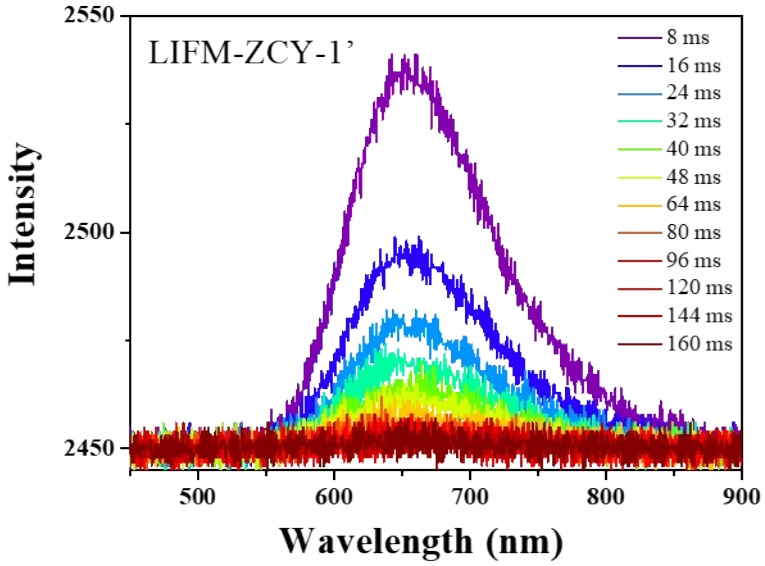

Figure S21. LPL spectra of LIFM-ZCY-1' at 300 K under 365 nm excitation.

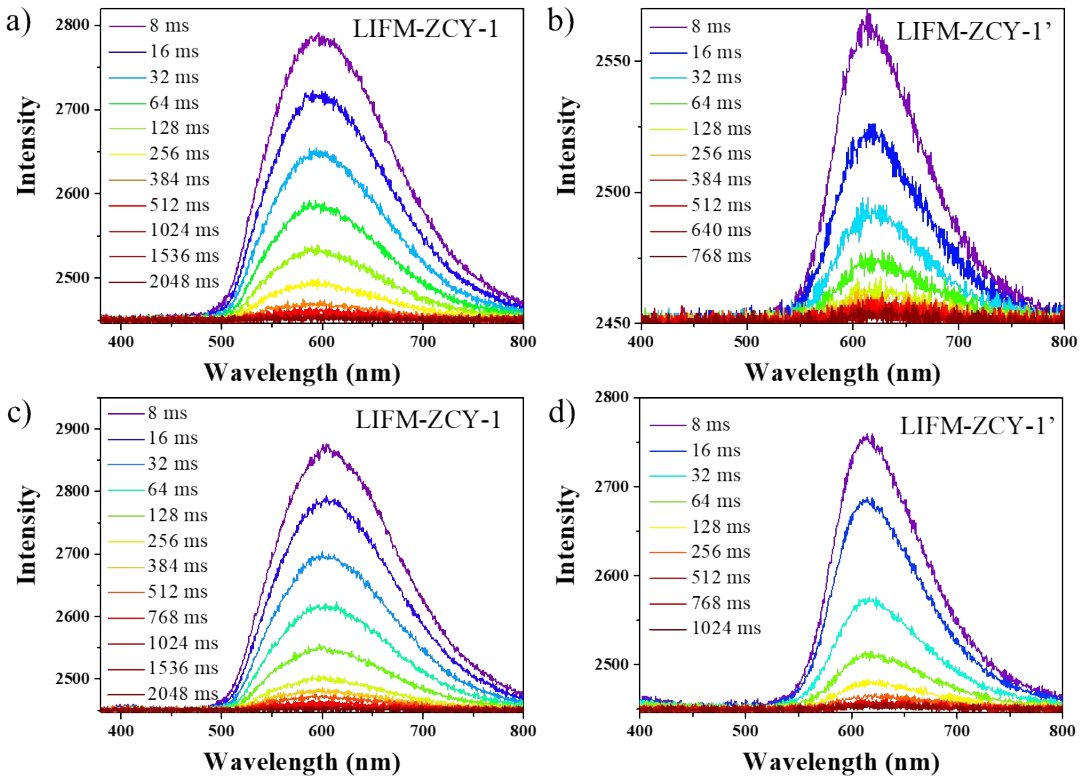

Figure S22. Low temperature (77 K) LPL spectrum of LIFM-ZCY-1 and LIFM-ZCY-1' under 365 nm (a-b) and 405 nm excitation (c-d).

Table S8. Photophysical properties of LIFM-ZCY-1 and LIFM-ZCY-1'.

Targets	λ_{Fluo} (nm)	λ_{Phos} (nm)	τ_{Fluo} (ns)	$\tau_{Phos}\,(ms)$ $(300\ K, Air)$	$\tau_{Phos}\,(ms)$ $(300\ K, Vacuum)$	Φ (%)
LIFM-ZCY-1	433	583	6.76	2.95	18.39	7.5
LIFM-ZCY-1'	438	620	18.10	8.48	35.03	8.0

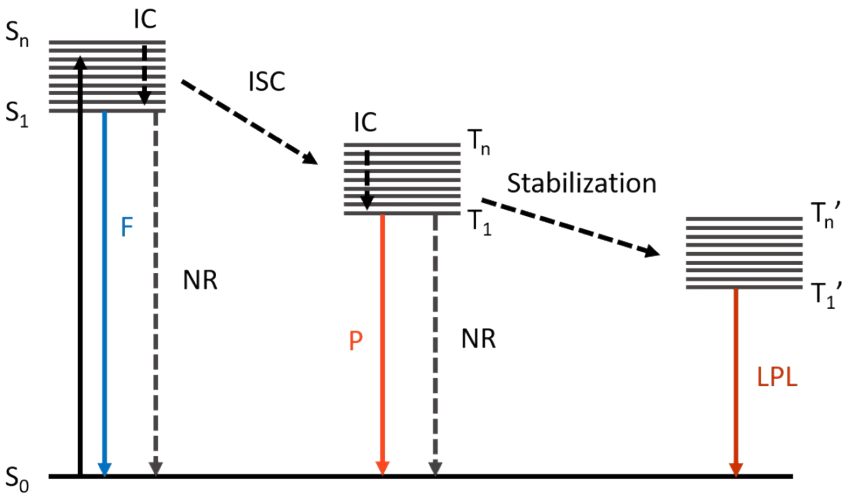

Scheme S2. Energy level diagram of the relevant photophysical processes for the phosphorescence and LPL of LIFM-ZCY-1'. F = fluorescence; P = phosphorescence;

S_0=ground state; S_1=lowest singlet excited state; S_n=high-level singlet excited state; T_1=lowest triplet excited state; T_n=high-level triplet excited state; T_n'=high-level stabilized triplet excited state; ISC=intersystem crossing; IC = internal conversion; and NR=nonradiative transition.

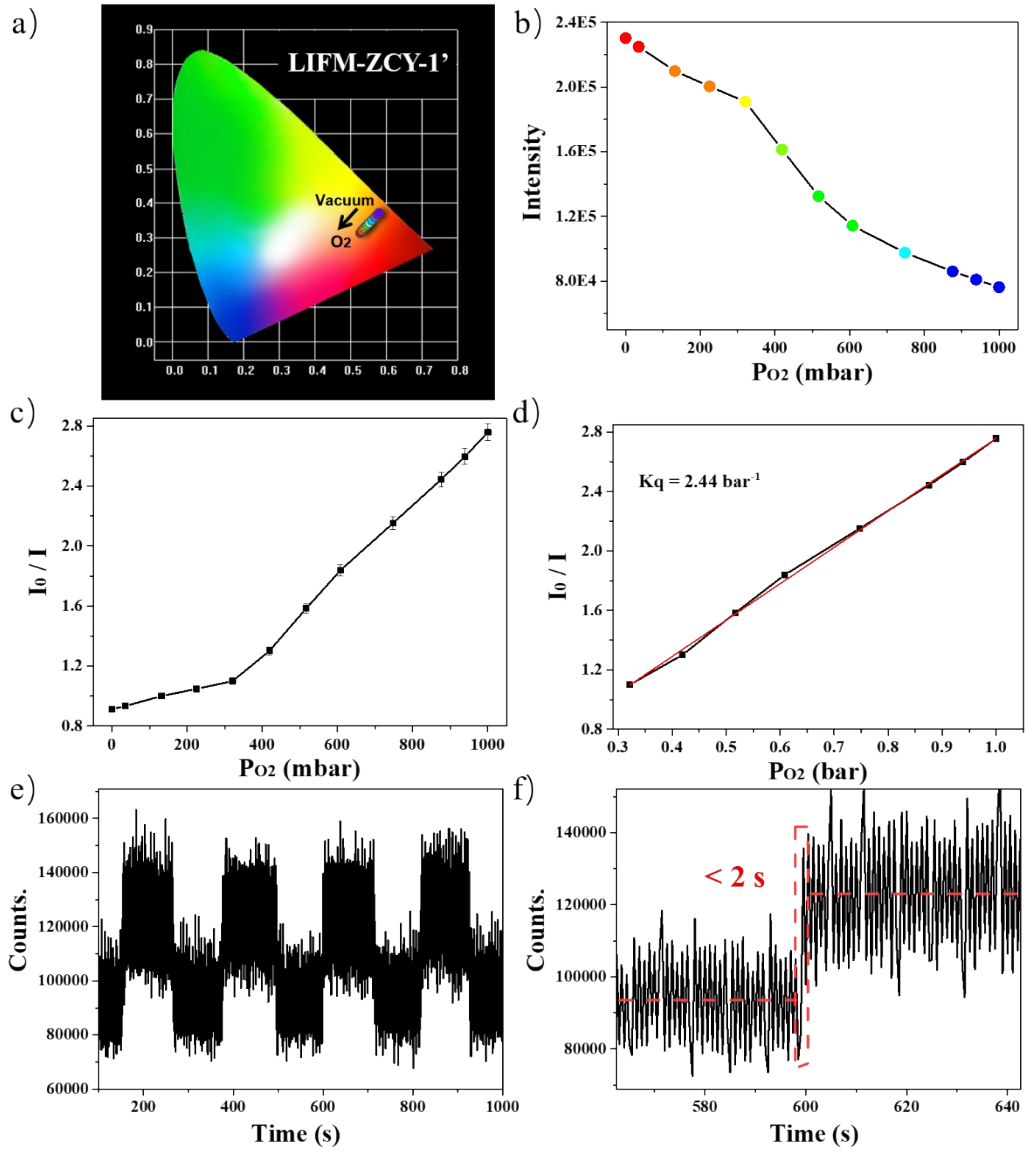

Figure S23. a) CIE coordinates of oxygen-dependent emission spectra of LIFM-ZCY-1' with 365 nm excitation. b) Oxygen-dependent emission intensity of LIFM-ZCY-1' at 620 nm, excitation at 365 nm. c-d) Stern–Volmer plot and linear correlation of the fluorescent/phosphorescent response to oxygen levels. e) Reversible oxygen sensing of emission intensity of LIFM-ZCY-1' at 620 nm in nitrogen- and oxygen-saturated atmosphere. f) Oxygen sensing of emission intensity of LIFM-ZCY-1' at 620 nm in nitrogen- and oxygen-saturated atmosphere, the response time is no more than 2s.

Table S9. Phosphorescence lifetime of LIFM-ZCY-1' under different oxygen content atmosphere.

P_{O2} (mbar)	Lifetime (ms)
0	35.03
25	26.48
49	20.47
69	14.78
126	10.02
189	8.87
300	8.06
460	7.23
754	5.69
1050	4.08

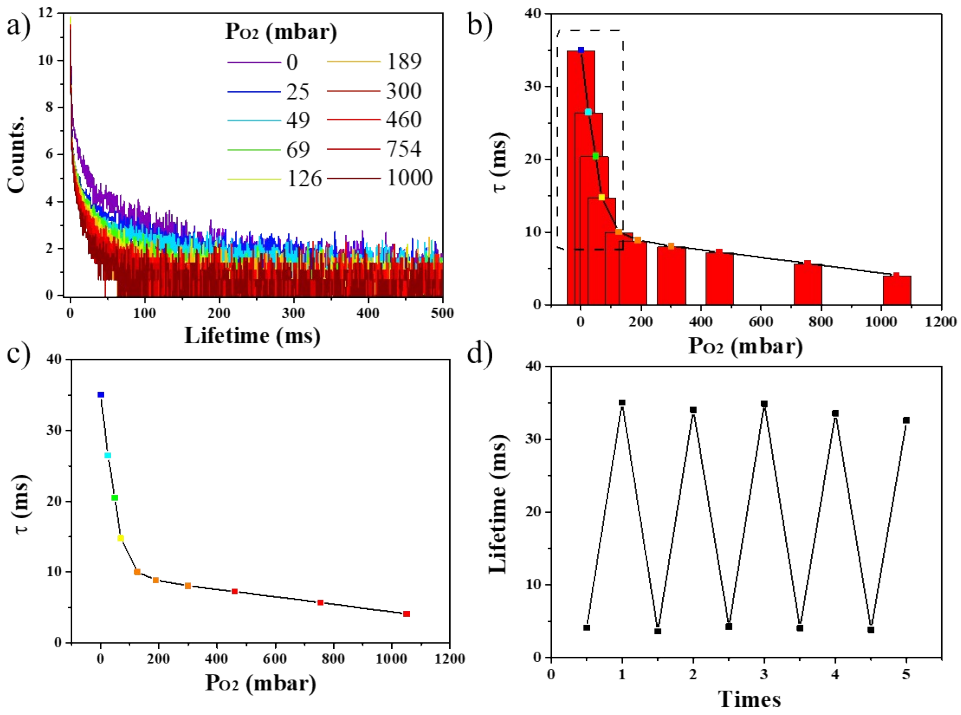

Figure S24. a) The decay curves of LIFM-ZCY-1' with varying oxygen fraction. b) Oxygen quenching diagram of LIFM-ZCY-1' in terms of phosphorescence lifetime at 620 nm. c) Fitted lifetime of LIFM-ZCY-1' with varying oxygen fraction. d) Reversible oxygen sensing of lifetime at 620 nm of LIFM-ZCY-1' in nitrogen- and oxygen-saturated atmosphere.

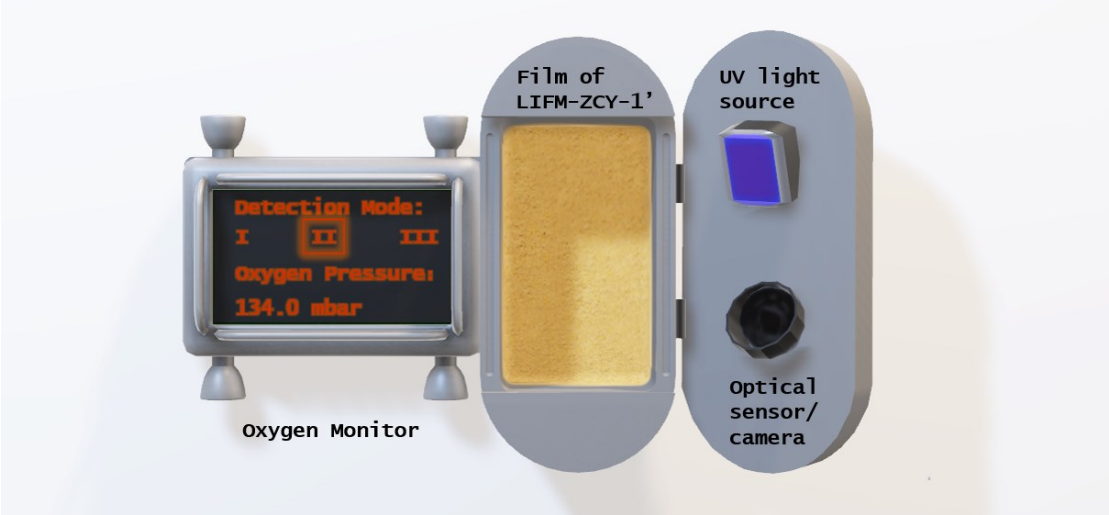

Figure S25. Schematic diagram of multi-mode oxygen sensing device with LIFM-ZCY-1' film. Ideally, the device can be set up to three detection modes, 300-1000 mbar (based on emission intensity), 0-150 mbar (based on lifetime), and ultra-low (< 8 mbar, based on LPL).

References

[S1] Becke, A. D. *J. Chem. Phys.* **1993**, *98*, 5648–5652.

[S2] Lee, C.; Yang, W.; Parr, R. G. *Phys. Rev. B*, **1988**, *37*, 785–789.